Neural Operator Learning for Ultrasound Tomography Inversion

Haocheng Dai*, Michael Penwarden*, Mike Kirby, Sarang Joshi. (*equal contribution)

MIDL 2023

Top 10 Cancers by Rates of New Cancer Cases
United States, 2016-2020, All Races and Ethnicities, Female

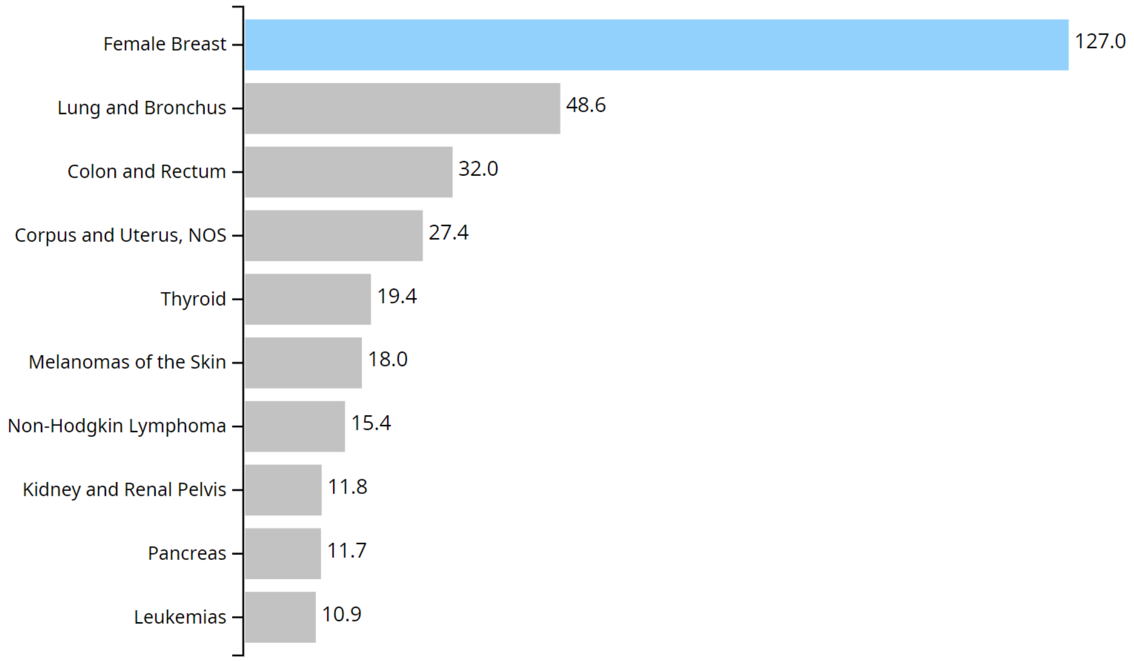

Top 10 Cancers by Rates of Cancer Deaths
United States, 2016-2020, All Races and Ethnicities, Female

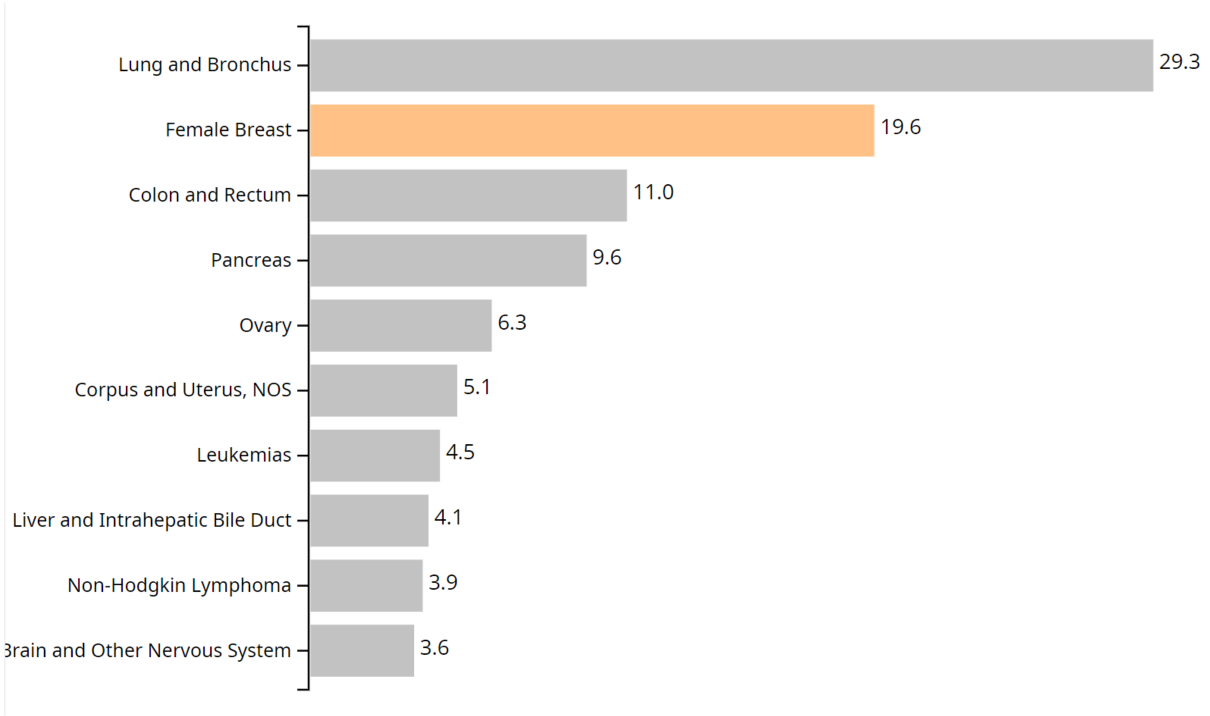

More women are diagnosed with breast cancer than any other type of cancer.
More woman are died from breast cancer than any other type of cancer, besides lung cancer.

Source - U.S. Cancer Statistics Working Group. U.S. Cancer Statistics Data Visualizations Tool, based on 2022 submission data (1999-2020): U.S. Department of Health and Human Services, Centers for Disease Control and Prevention and National Cancer Institute; https://www.cdc.gov/cancer/dataviz, released in November 2023.

The 5-year survival rate for breast cancer stands at 90%, yet this rate is closely tied to the (1) timing of detection and (2) treatment.

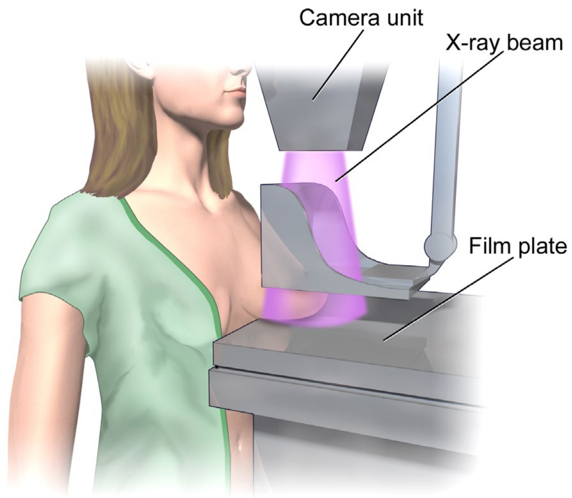

Mammograms (X-ray)

50% of women between the ages of 40-74 in the US have dense breasts.

❌ Mammograms misses 35.6–52.2% of breast cancers in dense breast tissue.

MRI

✅ works well on extremely dense breast tissue.

❌ high expenses, hard accessibility, and high false positive rates.

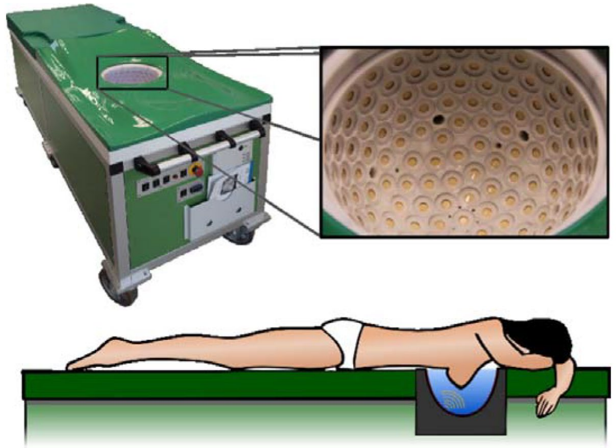

Ultrasound

✅ low expenses, radiation free

✅ can detect tiny, node-negative breast tumors

✅ can be used in treatment

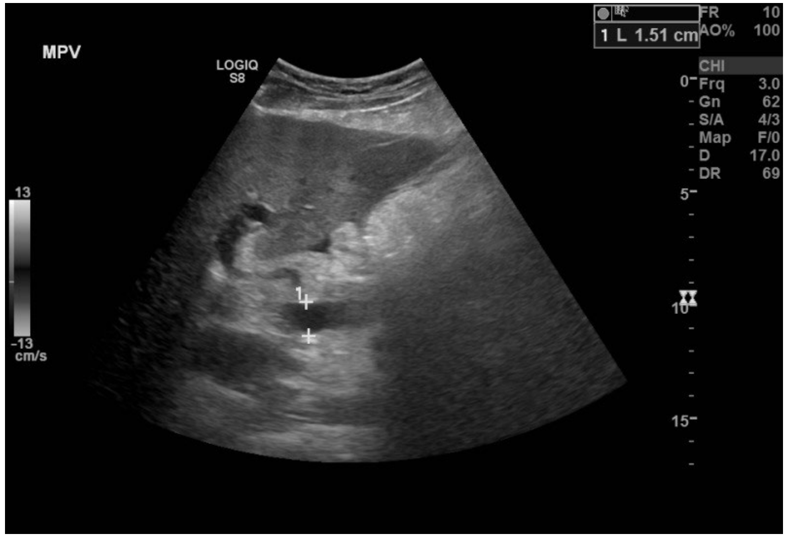

B-mode Ultrasound

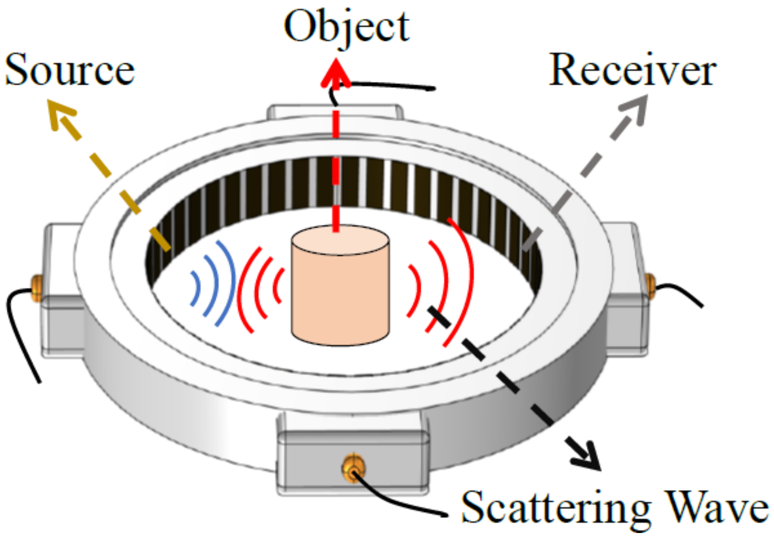

Ultrasound Computed Tomography

The 2D scalar wave equation in the homogeneous medium can be denoted as

$$\underbrace{\frac{\partial^2 p(\mathbf{x},t)}{\partial \mathbf{x}_1^2}}_{} + \frac{\partial^2 p(\mathbf{x},t)}{\partial \mathbf{x}_2^2} - \frac{1}{c(\mathbf{x})^2} \cdot \frac{\partial^2 p(\mathbf{x},t)}{\partial t^2} = 0$$

pressure

spatial position

temporal position

speed of sound

In steady-state conditions, namely the source pressure is periodic and never fades out, we can Fourier-transform the pressure in time to

$$p(\mathbf{x}, t) = \int_{-\infty}^{\infty} p(\mathbf{x}, \omega) e^{-j\omega t} d\omega$$

By substituting the Fourier-transformed pressure into the wave equation, we have

$$\nabla^2 p(\mathbf{x}, t) - \frac{1}{c(\mathbf{x})^2} \cdot \frac{\partial^2 p(\mathbf{x}, t)}{\partial t^2} = 0$$

wave equation

$$\nabla^2 \left(\int_{-\infty}^{\infty} p(\mathbf{x}, \omega) e^{-j\omega t} d\omega \right) - \frac{1}{c(\mathbf{x})^2} \cdot \frac{\partial^2}{\partial t^2} \left(\int_{-\infty}^{\infty} p(\mathbf{x}, \omega) e^{-j\omega t} d\omega \right) = 0$$

$$\int_{-\infty}^{\infty} \left[\nabla^2 \left(p(\mathbf{x}, \omega) e^{-j\omega t} \right) - \frac{1}{c(\mathbf{x})^2} \cdot \frac{\partial^2}{\partial t^2} \left(p(\mathbf{x}, \omega) e^{-j\omega t} \right) \right] d\omega = 0$$

$$\int_{-\infty}^{\infty} \left[e^{-j\omega t} \nabla^2 p(\mathbf{x}, \omega) - \frac{p(\mathbf{x}, \omega)}{c(\mathbf{x})^2} \cdot \frac{\partial^2}{\partial t^2} \left(e^{-j\omega t} \right) \right] d\omega = 0$$

$$\int_{-\infty}^{\infty} \left[e^{-j\omega t} \nabla^2 p(\mathbf{x}, \omega) - \frac{p(\mathbf{x}, \omega)}{c(\mathbf{x})^2} \cdot \left(-\omega^2 e^{-j\omega t} \right) \right] d\omega = 0$$

$$\int_{-\infty}^{\infty} \left[\nabla^2 p(\mathbf{x}, \omega) + \frac{\omega^2}{c(\mathbf{x})^2} \cdot p(\mathbf{x}, \omega) \right] e^{-j\omega t} d\omega = 0$$

$$\nabla^2 p(\mathbf{x}, \omega) + \frac{\omega^2}{c(\mathbf{x})^2} \cdot p(\mathbf{x}, \omega) = 0$$

Helmholtz equation

The central goal of USCT is to reconstruct the spatial distribution of sound speed within biological tissues, denoted by $c(x)$, using the measurements obtained from the transducers, represented by y. This inverse problem can be formulated as a PDE-constrained optimization problem:

$$\min_{c(x),u_k(x)} L = \sum_{k=1}^{M} L_k = \sum_{k=1}^{M} \|y_k - u_k(x_f)\|_2^2$$

$$s.t. \left[\nabla^2 + \left(\frac{\omega}{c(x)}\right)^2\right] u_k(x) = -\rho_k(x).$$

This inverse problem is commonly referred to as frequency domain full waveform inversion (FD-FWI). Akin to many other inverse problems, FD-FWI is typically solved using gradient-based optimizers, but it can be computationally challenging for large-scale problems like 3D reconstructions.

Can we find a data-driven method in the era of deep learning to solve USCT problem? Namely learning a mapping between complex function spaces.

K-Wave simulator

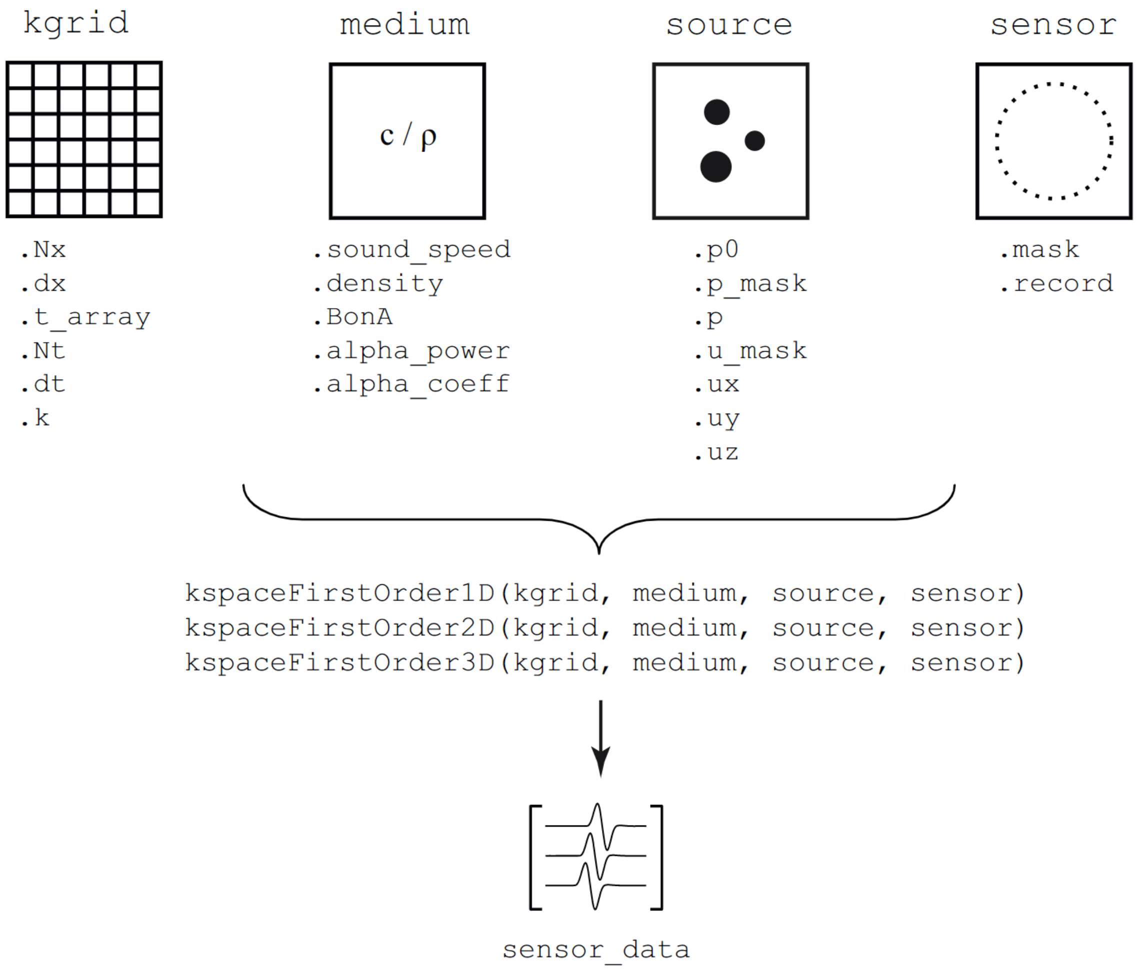

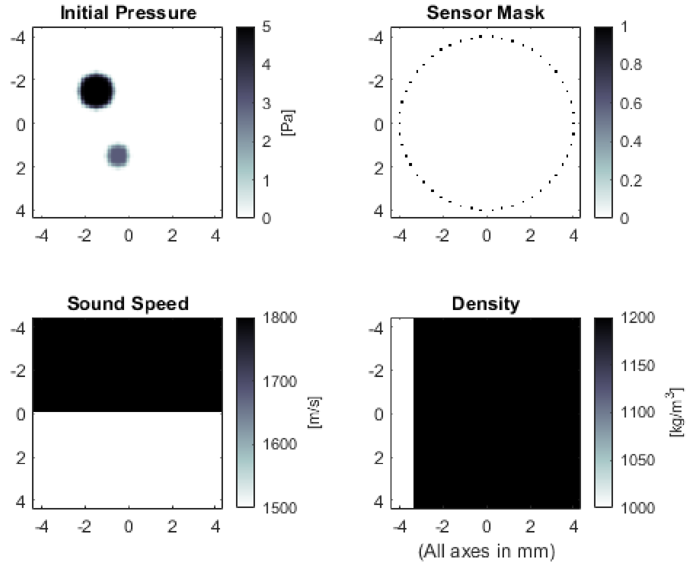

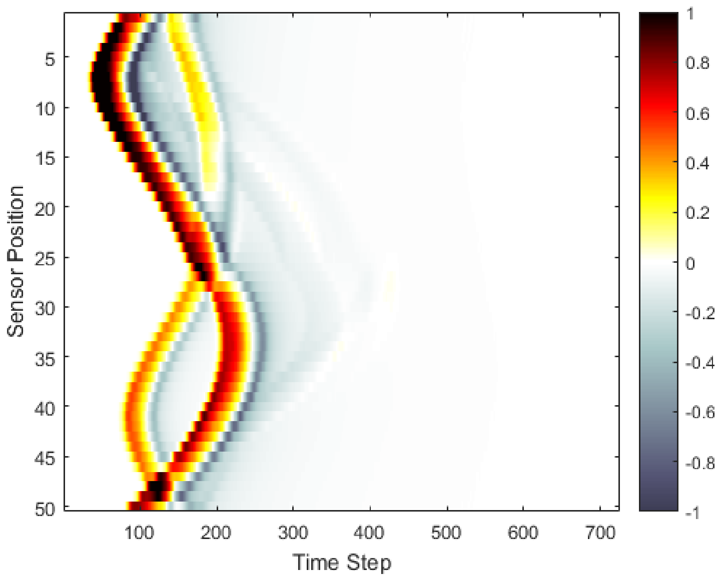

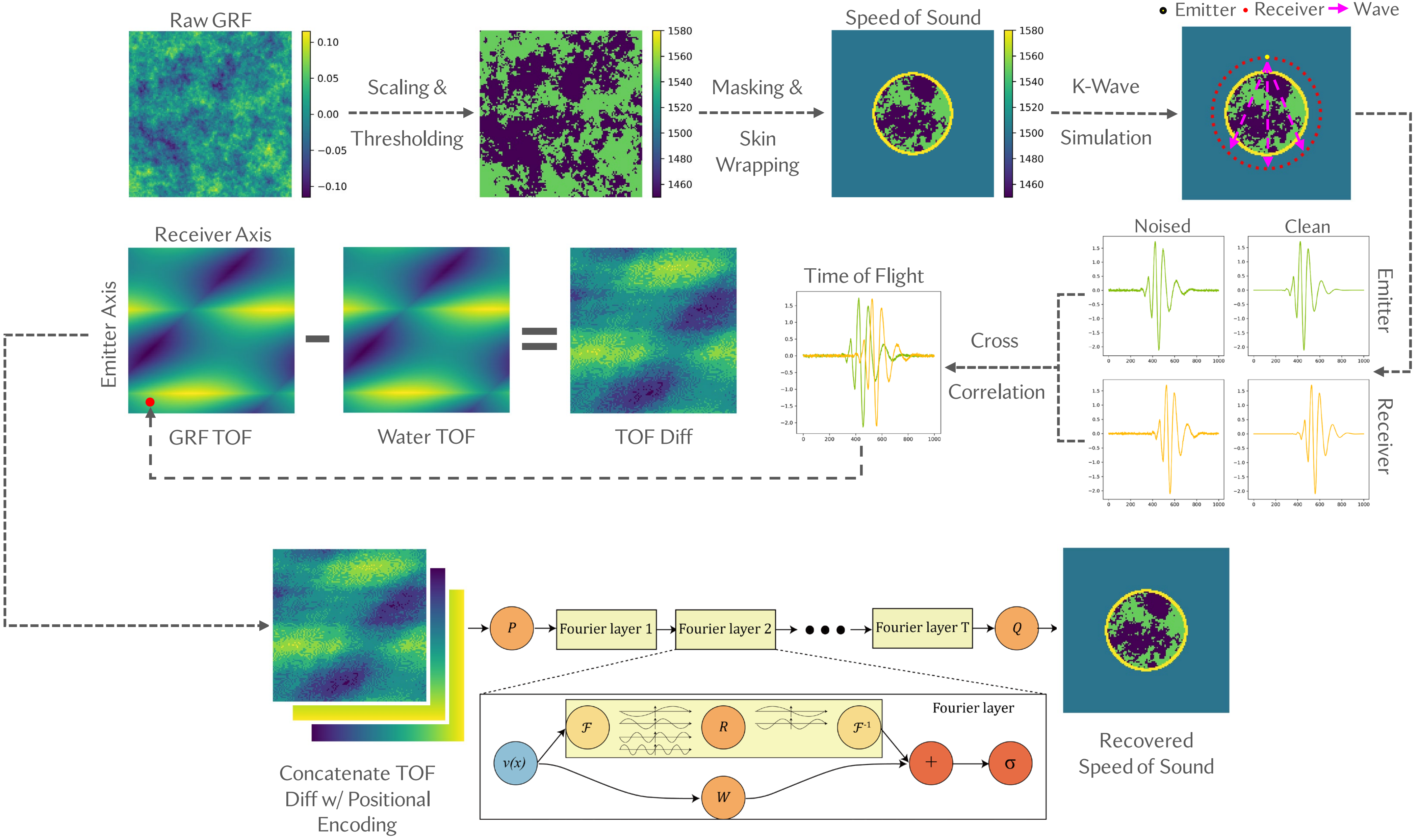

Raw GRF
Scaling &
Thresholding
Masking &
Skin
Wrapping
Speed of Sound
K-Wave
Simulation
Emitter
Receiver
Wave
Noised
Clean
Emitter
Receiver
Cross
Correlation
Time of Flight
Receiver Axis
Emitter Axis
GRF TOF
Water TOF
TOF Diff
Concatenate TOF
Diff w/ Positional
Encoding
P
Fourier layer 1
Fourier layer 2
Fourier layer T
Q
Fourier layer
v(x)
R
W
σ
Recovered
Speed of Sound

Single realization of train/test set examples

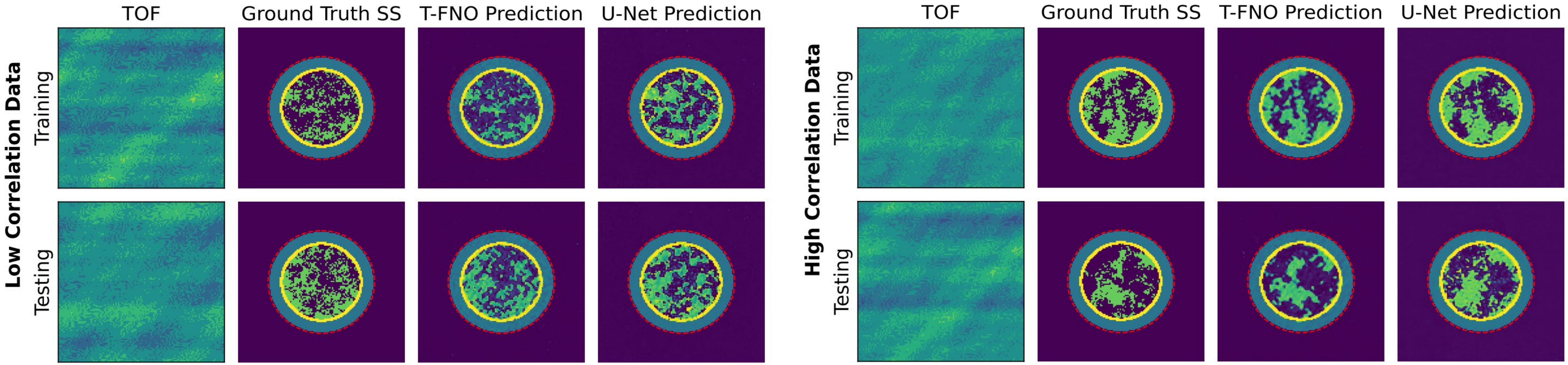

T-FNO better captures the structure feature in the phantom, compared to U-Net.

The dashed red line indicates the location of the evenly distributed emitters and receivers. The region outside the transducer ring is masked out for improved training and quantity of interest comparison but is present in the full-wave simulation to mitigate reflection.

MSE comparison between T-FNO and U-Net

Model	GRF Correlation	Noise	Testing MSE	Training MSE
T-FNO	High	Clean	$\mathbf{2.01 \pm 0.33 \times 10^{-2}}$	$0.69 \pm 0.11 \times 10^{-2}$
		10%	$\mathbf{2.06 \pm 0.34 \times 10^{-2}}$	$0.68 \pm 0.11 \times 10^{-2}$
	Low	Clean	$\mathbf{3.27 \pm 0.16 \times 10^{-2}}$	$1.00 \pm 0.06 \times 10^{-2}$
		10%	$\mathbf{2.67 \pm 0.17 \times 10^{-2}}$	$1.53 \pm 0.08 \times 10^{-2}$
U-Net	High	Clean	$2.52 \pm 0.44 \times 10^{-2}$	$\mathbf{0.12 \pm 0.03 \times 10^{-2}}$
		10%	$2.79 \pm 0.42 \times 10^{-2}$	$\mathbf{0.01 \pm 0.01 \times 10^{-2}}$
	Low	Clean	$3.81 \pm 0.17 \times 10^{-2}$	$\mathbf{0.42 \pm 0.05 \times 10^{-2}}$
		10%	$4.02 \pm 0.21 \times 10^{-2}$	$\mathbf{0.02 \pm 0.01 \times 10^{-3}}$

T-FNO outperforms the U-Net at test time under all conditions, whereas the U-Net better fits the training set but does not generalize well.

Training loss plot

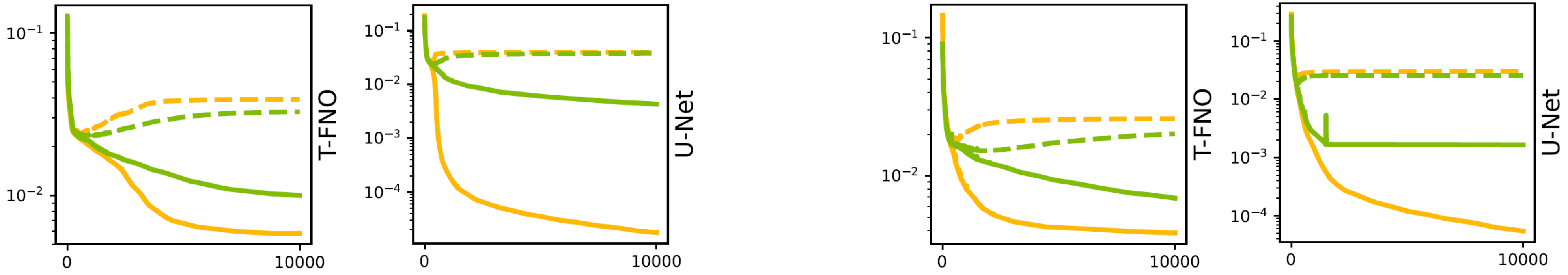

Low correlation data

High correlation data

Small training set Small testing set Big training set Big testing set

T-FNO better captures the overall trends in the data, while the U-Net is prone to overfit the training data.

The U-Net suffers from considerable generalization error, even when additional examples were provided.

Conclusions

1. We have proposed using neural operators to accurately and efficiently solve the full-wave inverse problem on synthetic ultrasound tomography.

2. Our novel application of the T-FNO improves over the baseline U-Net, laying the foundation for real-time accurate predictions of soft tissue distribution for tumor identification on breast imaging.

3. Additionally, the application of both U-Net and T-FNO to this problem formulation is itself novel since both are real-time predictors and do not require computationally expensive ray-based inversion once trained.